Soft Matter

PAPER

View Article Online
View Journal

Cite this: DOI: 10.1039/c8sm02590h

Soft thermal nanoimprint with a 10 nm feature size†

Ashish Pandey, Sivan Tzadka, Dor Yehuda and Mark Schvartzman *

Nanoimprinting with rigid molds offers almost unlimited pattern resolution, but it suffers from high sensitivity to defects, and is limited to pattering flat surfaces. These limitations can be addressed by nanoimprinting with soft molds. However, soft molds have been used so far with UV resists, and could not achieve a resolution and minimal feature size comparable to those of rigid molds. Here, we explore the miniaturization edge of soft nanoimprint molds, and demonstrate their compatibility with thermal imprint resists. To that end, we produced a pattern with 10 nm critical dimensions, using electron beam lithography, and used it to replicate nanoimprint molds by direct casting of an elastomer onto the patterned resist. We showed that the produced pattern can be faithfully transferred from the mold by thermal nanoimprinting. In addition, we showed that similar nanoimprint molds can also be produced by double replication, which includes nanoimprinting of a thermal resist with an ultrahigh resolution rigid mold, and replication of a soft mold from the imprint pattern. We also demonstrated our novel nanoimprinting approach in two unconventional applications: nanopatterning of a thermal resist on a lens surface, and direct nanoimprinting of chalcogenide glass. Our novel nanoimprint approach pushes the envelope of standard nanofabrication, and demonstrates its potential for numerous applications impossible up to now.

Received 21st December 2018,
Accepted 1st March 2019

DOI: 10.1039/c8sm02590h

rsc.li/soft-matter-journal

1. Introduction

Nanoimprint lithography was introduced more than 20 years ago,[1,2] and quickly became a popular nanopatterning method for numerous applications due to its unique combination of ultra-high resolution, high throughput, and pattern arbitrariness.[3–6] Originally, nanoimprint lithography was based on the embossing of softened polymer films with nanofabricated molds made of rigid materials, *e.g.* Si, SiO_2, or quartz.[7] Due to the stiffness of their relief features, rigid molds can replicate patterns whose resolution and minimal feature size have, in principle, no fundamental limitation. Indeed, Hua *et al.* used a solid substrate with ~2 nm thick carbon nanotubes as a nanoimprint mold and faithfully replicated the nanotube shapes within a thermal resist.[8] Also, nanoimprint molds fabricated by electron-beam lithography were shown to produce nanopatterns with a resolution down to a few nanometers.[9,10] This evidence clearly demonstrates that the resolution and minimal feature size of nanoimprinting with rigid molds are defined largely by the geometry of the mold relief features.

A popular alternative to rigid molds is soft elastomeric molds,[11–13] which can be replicated by casting of an elastomeric material onto a nanopatterned master. The material of choice for soft molds is polydimethylsilane (PDMS), which is also broadly used for microcontact printing.[14] Soft PDMS molds have a few advantages over their rigid counterparts. First, numerous soft molds can be replicated from one fabricated master. Second, soft nanoimprint molds are less sensitive to surface defects and contamination than rigid molds. Third, due to the low surface energy of PDMS, soft molds require no antiadhesive coating, which is necessary for silicon- or silica-based rigid molds. Fourth and finally, soft molds can be used to imprint curved substrates. However, the imprint resolution and feature size of standard PDMS molds are limited to a few hundred nanometers, because their soft relief features buckle and deform upon the pressure applied during the imprint process. To overcome this limitation, Schmid *et al.* formulated hard PDMS (h-PDMS) with an enhanced elastic modulus, and used it for high-resolution stamps for microcontact printing.[15] Later, Odom *et al.* combined an imaging layer for h-PDMS with a soft PDMS substrate into hybrid PDMS/h-PDMS molds to imprint features sized down to 50 nm.[16] Since then, additional hybrid soft molds have been reported, in which the mechanical properties of relief features were tuned to allow imprint resolution down to a sub-20 nm scale.[17–20]

Despite the impressive progress in the development of ultrahigh resolution soft nanoimprint molds, including patterning of sub-10 nm features,[21] they have been applied exclusively for UV nanoimprinting.[13] On the other hand, thermal nanoimprinting has

Department of Materials Engineering, Ilse Katz Institute for Nanoscale Science and Technology, Ben-Gurion University of the Negev, Beer-Sheva, 84105, Israel.
E-mail: marksc@bgu.ac.il

† Electronic supplementary information (ESI) available. See DOI: 10.1039/c8sm02590h

many important applications, *e.g.* direct embossing of thermoplastic substrates,[22] or direct patterning of functional polymeric materials,[23] such as electrochromic polymers in displays,[24] photovoltaic polymers in solar cells, or fluorescent polymers in sensors.[25] However, thermal nanoimprinting has been traditionally realized with rigid molds. Notably, thermoplastic polymer films can be patterned with elastomeric molds by capillary force lithography, in which a PDMS mold is placed on a polymer film and heated above its glass transition point, allowing the polymer to melt and fill the void spaces by capillary force.[26] Although this process shares similar features with nanoimprinting, it is much more time-consuming: a typical patterning by capillary force lithography takes from a few hours to several tens of hours, due to extremely slow capillary flow of the viscous polymer melt.[27] Furthermore, capillary force lithography of a thermoplastic polymer with a PDMS mold is limited to producing features at the micron scale.[28] Recently, we reported a fast and high-resolution patterning of a thermoplastic polymer using a nanocomposite mold consisting of a soft substrate and rigid relief features.[29] However, such molds are fabricated by a complex process that includes electron beam lithography, pattern transfer from a sacrificial layer to PDMS, and application of an antiadhesive coating.[30] Facile and reliable approaches for thermal imprinting with nanoscale resolution using soft molds are still to be explored.

Patterning of polymer films with soft stamps has been recently demonstrated, however, it has been limited to micron-scale resolution.[31] Here, we show, for the first time to the best of our knowledge, that soft elastomeric molds can be used to pattern thermoplastic resists with nanoscale resolution and feature size, and by this we push the miniaturization limits of soft nanoimprint lithography to an unprecedented level. In the context of miniaturization, it is very important to stress the difference between minimal feature size and resolution, which is defined as the minimal spacing between lithographically produced features. Features of a few tens of nm resolved by a spacing below 10 nm have been recently fabricated by soft imprinting of sol–gel resists.[32] However, features of 10 nm dimensions imprinted with soft molds have not been reported before, as far as we know. Remarkably, the resolution limits of soft nanoimprinting are often associated with the insufficient stiffness of the soft mold and the viscosity of the used resist. Here, we hypothesized that the miniaturization abilities of soft nanoimprint lithography are bottlenecked by the minimal size and resolution of the features on the master, rather than by the properties of the mold and resist materials. We prove our hypothesis by fabricating master molds nanopatterned with features whose dimensions were as small as 10 nm, and faithfully transferred these features into the replicated soft mold, and then to a thermal resist by nanoimprinting.

In this paper, we present two possible routes for fabricating ultra-high-resolution master molds. One route is based on the direct patterning of a thin polymer film by electron beam lithography, with no further pattern transfer. The second route harnesses hydrogen silsesquioxane (HSQ) – a negative electron beam resist with the highest possible patterning resolution. Here, an ultra-high-resolution hard mold is first produced by direct pattering of HSQ, and then is replicated onto a thin thermoplastic film to produce a master mold. We used both types of masters to produce soft molds for the thermal nanoimprinting of a thermoplastic polymer. In addition, we demonstrated here two unconventional applications of soft thermal nanoimprinting. In the first application, we produced thermally imprinted ultrahigh resolution nanopatterns in a resist film on top of a curved optical lens. In the second application, we directly imprinted the surface of chalcogenide glass. Remarkably, the latter application is an important milestone in the emerging field of direct nanoimprinting of inorganic materials, and here we demonstrated the smallest features produced by direct imprinting of inorganic materials. Overall, our findings provide new important insights into the miniaturization capabilities of soft nanoimprint lithography, and pave the way to its numerous applications impossible up to now.

2. Materials and methods

2.1 Fabrication of soft molds

We first produced a master using ultra-high-resolution patterning of a positive tone electron-beam resist (ZEP, Zeon Inc, thickness 30 nm) on a Si substrate. We then produced h-PDMS/PDMS soft molds by directly casting their precursors onto the electron-beam patterned resist. For this purpose, we first mixed 3.4 g of vinyl PDMS prepolymer (VDT-731, Gelest corp), 18 μL of platinum catalyst (platinum divinyltetramethyldisiloxane, SIP6831.2LC Gelest Corp.) and 5 μL of modulator (2,4,6,8-tetramethyl tetravinylcyclotetrasiloxane, Sigma-Aldrich) and degassed the mixture for 1–2 min.[15,16] We then gently added 1 g of hydrosilane prepolymer (HMS-301, Gelest Corp.) to the mixture, gently stirred it, immediately applied a thin film of the resulting new mixture onto the master by spin coating, and cured it at 60 °C for 30 min. After cooling the cured film, we poured onto it a mixture of PDMS (Sylgard 184 PDMS, Dow Corning) and its hardening reagent (10 : 1 v/v), degassed it, and further baked at 60 °C for 1 h. Finally, we peeled the obtained mold off the master. We scanned the fabricated PDMS molds with Atomic Force Microscopy (AFM) (MFP-3D-Bio, Asylum Research).

2.2 Mold fabrication by double replication

The double replication method included fabrication of a hard nanoimprint mold by electron beam patterning of HSQ on a silicon substrate. We first spin-coated a thin film of HSQ (XR-1541, Dow Corning) on a silicon wafer and patterned it by electron beam lithography, using AZ 726 (Rohm and Haas) as a developer. For complete transformation of e-beam-exposed HSQ to nonstoichiometric silicon oxide, we annealed it at 550 °C for 1 h, and ashed in oxygen plasma for 1 min. We then immersed the obtained rigid mold into a commercial mold-release agent [NXT-110A, diluted in NXT-110B 1 : 50 v/v (Nanonex)] for 2 min inside a glovebox, and rinsed with acetone. We used the HSQ mold to imprint a poly(benzyl methacrylate) (PBMA, Sigma-Aldrich) resist. For this process we first spin coated a thin film of PBMA diluted in anisole onto a Si substrate, and baked it at 120 °C

for 2 min. We performed the nanoimprinting using a commercial imprinting tool (Nanonex, NX-B200) at 2.8 MPa and 100 °C for 4 min. Finally, we cast the mold on the imprinted resist surface using the procedure described in the previous section.

2.3 Thermal nanoimprinting on both a flat and a curved substrate (lens)

To demonstrate the compatibility of our PDMS/h-PDMS mold with imprinting on flat and curved substrates, we chose PBMA as a thermal resist. PBMA was diluted in toluene, spin-coated on both flat and curved surfaces, and baked at 100 °C for 2 min. For the high-resolution patterns, the resist thickness was 60 nm, and its uniformity on both the flat and curved samples was verified by AFM and profilometry. The nanoimprinting was carried out using a commercial imprinting tool (Nanonex, NX-B200). The imprinted substrate with the mold on top was placed between two elastic membranes, and the space between the membranes was pumped out to prevent bubbles in the imprinted polymer. The imprint temperature, pressure and time were 100 °C, 340 kPa, and 5 min respectively. The pressure was applied after the temperature reached its setpoint. The imprinted pattern was inspected using Scanning Electron Microscopy (SEM, Verios XHR 460L SEM).

2.4 Nanoimprinting on chalcogenide glass

We directly imprinted substrates of As_2Se_3 (1 mm thick and 2.54 cm in diameter) using a custom-made thermal nanoimprint setup described previously[33] (Fig. S1, ESI†). Briefly, we placed on a hot plate a metallic ring, whose inner diameter and height were 2.55 cm and 3.38 cm, respectively. The purpose of the ring was to confine the chalcogenide glass, and prevent it from flowing sideways, due to the applied imprinting force. We then placed the soft mold cut to a diameter of 2.54 cm within the ring, with the patterned surface up, and placed on top of it the As_2Se_3 substrate. To conserve a high-quality surface finish, we placed smooth BK7 glass (a diameter of 2.54 cm and a thickness of 1 mm) in contact with the back surface of the chalcogenide glass, and a metal disc on top of BK7. Finally, we covered the assembly with a silicone membrane, and sealed it with a high-pressure chamber. During the imprinting, we pumped the air out of the space beneath the membrane, heated the plate, and applied high pressure to the chamber. After completing the imprint, the setup was cooled down to room temperature before its disassembly. The used temperature, pressure and imprint time were 215 °C, 90 kPa, and 15 min, respectively.

3. Results and discussion

In this work, we explored ultra-high resolution soft thermal nanoimprinting using two types of master molds. The first type was produced by direct patterning of a polymeric resist film on a Si substrate using electron beam lithography (Fig. 1a). To explore the feature size limits of thermal soft nanoimprinting, we patterned the master mold with a variety of shapes whose critical dimensions were sized down to 10 nm. We used this

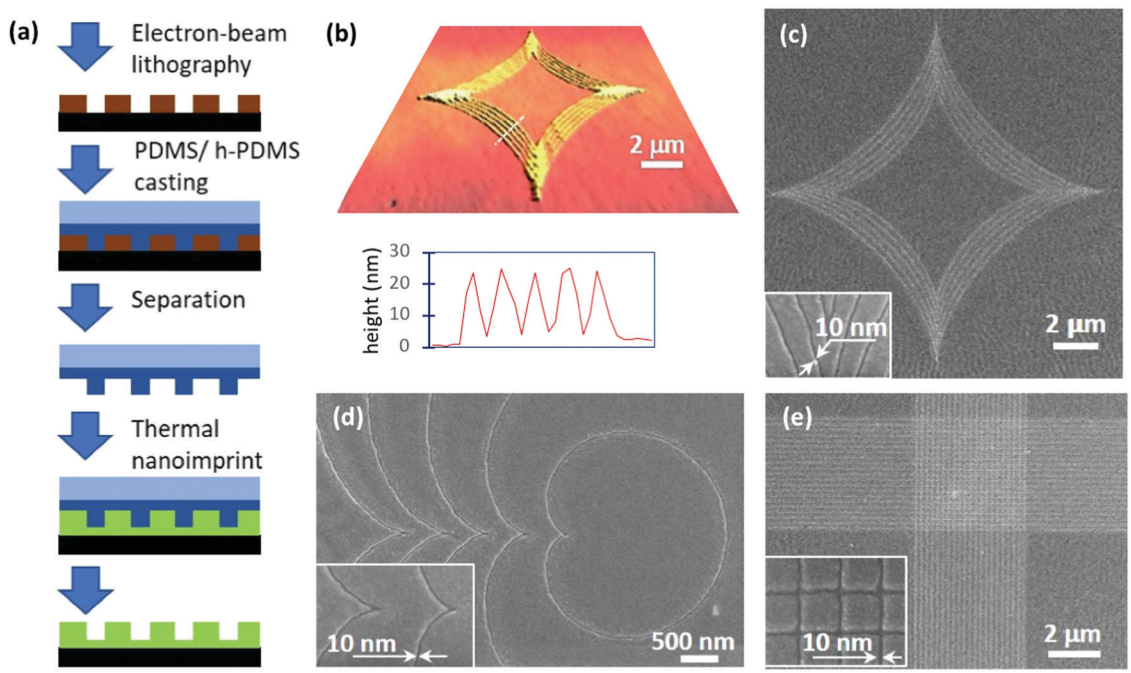

Fig. 1 (a) Process flow showing nanoimprinting using a hybrid PDMS mold on a substrate coated with a thermal resist. (b) AFM image of a pattern on a replicated soft mold, and cross section profile of the patterned lines. (c) SEM image of the same pattern transferred to a thermal resist. (d and e) SEM images of two additional patterns. Note: the wrinkles in the high-magnification SEM images are the result of localized charging and heating of the imprinted polymer film during the imaging. Whereas using a low-energy beam could, in principle, partially prevent this charging, it did not provide sufficient imaging quality. Also, discharging metallic films, which are commonly deposited to prevent such charging, would substantially distort the imprinted features with 10 nm dimensions, and thus could not be used in this case.

master to replicate h-PDMS/PDMS soft molds, whose nanoimprint reliefs were then characterized by AFM (Fig. 1b). We used the obtained soft molds for the thermal nanoimprinting of thin polymer films on Si substrates. It can be clearly seen that thermal nanoimprinting can faithfully reproduce shapes such as ultra-thin lines, 2D grids, and curves, with minimal critical dimensions down 10 nm (Fig. 1c–e). We found that the obtained imprinted nanopatterns fully reproduce the original patterns on the electron-beam written master (Fig. S2, ESI†). We inspected the imprinted patterns at different locations on the sample, and verified the uniformity of the pattern transfer (Fig. S3a, ESI†). We also verified the sub-10 nm minimal feature size of the imprinted pattern by measuring the full width half maximum of the perpendicular profile of the imaged lines[34] (Fig. S4, ESI†).

We would like to highlight several important aspects of the obtained results. The first aspect is related to the fact that soft molds have been traditionally used to imprint UV curable resists. Our findings clearly demonstrate that soft molds can also be used for high-resolution thermal nanoimprinting. This application of soft molds has been unexplored up to now. Notably, remarkable advantages of thermal nanoimprinting over its UV-based counterpart include the very broad variety of thermoplastic materials that can be imprinted, as well as the fact that thermal resists can be spin-coated with a uniform and highly controllable thickness, whereas liquid UV resists are mostly dispersed on the surface with low thickness uniformity.

The second aspect is related to the way we produced our master. Traditionally, masters for casting PDMS molds and their hybrid variations are fabricated by lithography and plasma etching (see, for example, ref. 35). This fabrication approach has several limitations. First, controlling the depth of the plasma-etched features is challenging due to micro-loading effects, especially for pattern elements sized below 100 nm.[36] Second, due to the partial isotropic nature of plasma etching, it often broadens the etched features, and creates their irregular non-vertical profiles, which have often conical or bottle-like shapes.[37] Finally, if a pattern is heterogeneous and non-periodic, the etched depth and profile will vary across the pattern and depend on the size and shape of each feature, as well as on their proximity to other features. All these characteristics of plasma etching substantially challenge the fabrication of masters for soft lithography and limit the fidelity of the pattern transferred by nanoimprinting.

Interestingly, direct replication of a soft mold from electron-beam patterned HSQ has been previously demonstrated.[38] There, HSQ, which is a negative-tone electron beam resist, was patterned in the form of nanosized posts, so the replicated soft mold consisted of an array of nano-pits. Furthermore, HSQ is an inorganic material, which, after being exposed to an electron beam, turns into a hard material with a structure and properties close to those of porous silica.[39] Conversely, here we demonstrate that an organic, positive-tone electron-beam patterned resist can be directly used as a master for the replication of ultra-high-resolution soft molds. Such a master overcomes all the above-listed limitations of plasma etched masters, since the height of its relief features is determined by the resist thickness, and therefore is uniform and independent of the feature shape and size. Furthermore, the profile of the mold features replicated from our master depends on the contrast of the electron-beam resist, as well as the conditions used for its development, and can be completely vertical.

The third aspect is related to the achieved critical dimension of the imprinted features. Remarkably, rigid molds can yield a minimal feature size and resolution of 10 nm and even below.[40,41] At the same time, the miniaturization limits of soft molds have remained for many years at the 50 nm level,[42] and the addition of a hardened imaging layer to soft elastomeric molds allowed the fabrication of features sized down to 15 nm.[18] Here, we demonstrated that hybrid PDMS molds can replicate features with critical dimensions of 10 nm – nearly as small as what can be achieved by rigid molds. Based on these findings, we conclude that the produced feature size allowed by soft nanoimprinting is bottlenecked by the dimensions of the master used to replicate the mold, and can, in principle, reach a sub-10 nm scale given the ability to fabricate a master with sub-10 nm features. It should be noted that the molds used in this work maintained their pattern geometry for up to 10 imprints. This finding is evidence of the high durability of our mold in thermal imprinting.

Fabrication of master molds with 10 nm features is at the cutting edge of electron beam lithography. For master molds based on patterned polymeric resists, such as those described in the previous section, achieving such a fine feature size requires an extremely tight window of the process parameters. Furthermore, electron beam patterning of organic polymers is highly sensitive to their molecular weight. A more reliable and robust approach for ultra-high-resolution electron beam patterning is based on hydrogen silesquioxane (HSQ) – an inorganic resist with the best resolution, critical dimensions, and contrast.[43,44] Remarkably, HSQ can be patterned by electron beam lithography and annealed to fabricate nanoimprint molds, with no need for pattern transfer to the substrate by plasma etching.[45–48] In this case, the height of the obtained HSQ features is highly uniform since it is determined by the thickness of the HSQ resist. However, fabrication of HSQ nanoimprint molds by electron beam lithography is often time consuming and expensive. Also, these molds are susceptible to mechanical deterioration upon multiple imprint cycles, and thus have a limited lifetime. The combination of these two constraints makes HSQ molds unsuitable and cost-ineffective for high-volume nanofabrication.

Here, we demonstrate that HSQ based nanoimprint molds can be harnessed for ultra-fine soft thermal nanoimprinting, using a double mold replication process (Fig. 2a). In this process, we first produced a rigid mold by pattering a silicon substrate with HSQ, and then imprinted it into a thermal resist. We then used the patterned resist as a master, onto which we cast a hybrid PDMS mold. Fig. 2b–f show micrograph images of the rigid Si-HSQ mold, which consists of an array of 20 nm HSQ nanodots, its replica in a thermal resist, and a thermal nanoimprint made by the soft mold replicated from the patterned thermal resist, respectively. The obtained results clearly show that HSQ relief features can be transferred throughout the

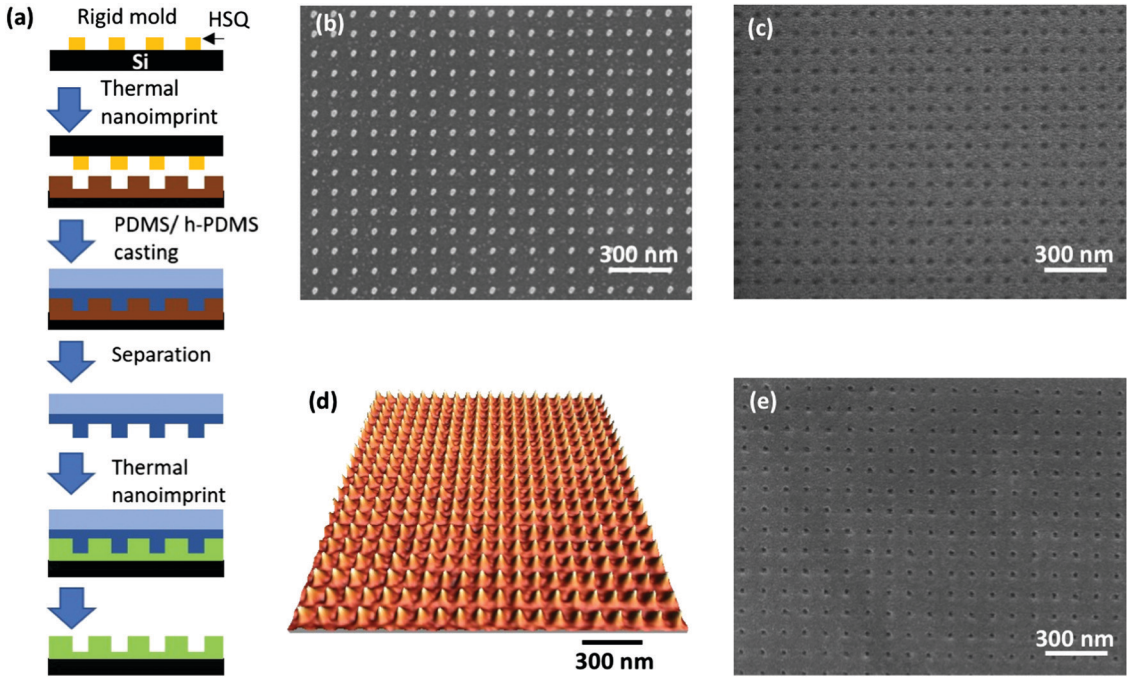

Fig. 2 (a) Process flow of soft mold fabrication by the double replication method. (b) SEM of a pattern on a HSQ rigid mold, which consists of an array of 20 nm nanodots. (c) The same pattern transferred from the rigid mold to a thermal resist. (d) AFM of a soft mold replicated from the previous pattern. (e) Thermal imprint of the soft mold produced in the previous stage.

multiple steps to finally obtain nanopatterns in the thermal resist, with excellent pattern fidelity and critical dimensions down to 20 nm. Notably, this nanofabrication process greatly benefits from the fact that the original HSQ mold can be used once to produce a replica, which in turn can be used to produce multiple soft molds. Naturally, each soft mold by itself can be used for multiple thermal imprints. Thus, this approach for soft nanoimprinting substantially increases the lifetime of the original HSQ mold.

Combining a soft mold and a thermal imprint resist is quite unusual, and while determining its process parameters, several aspects should be considered. The first one is related to the resist viscosity. Unlike UV resists, which are commonly used in soft imprinting, and whose viscosity is quite low – 10^{-2}–10^{-3} Pa s, the viscosity of softened thermoplastic resists is temperature dependent, and is in the range of 10^{3}–10^{7} Pa s.[49] Because the time for the complete filling of the mold cavities is linearly proportional to the temperature-dependent viscosity, and inversely proportional to the applied pressure,[50] elevated temperature and pressure facilitate achieving complete imprinting within a reasonable process time, as is commonly done with a rigid mold. In soft molds, however, the applied pressure has a negative side effect: it deforms the relief features, and the degree of deformation increases with the pressure.[51–53] Thus, achieving full imprinting while keeping the high fidelity of the transferred pattern could be quite challenging for thermal imprinting with soft molds, and would likely require a narrower process window than that allowed in thermal imprinting with a rigid mold.

To experimentally examine the allowed process window for thermal imprinting with a soft elastomer mold, we produced a test soft mold patterned with a series of gratings, whose period ranged from 1 micron to 4 microns, and whose feature height was 250 nm. We carried out the imprinting at several temperatures above the glass transition point of the same resist used previously, which is 54 °C, while keeping the imprint pressure and time at 340 kPa and 5 min, respectively. We found that for the imprinting process done at 80 °C, the imprinted feature height was around 40 nm – substantially lower than the feature height on the mold. Increasing the temperature led to increasing the imprint depth, as well as a change of the imprint profile (Fig. S5 and S6, ESI†). We believe that this profile change stems from the gradual decrease in both the resist viscosity[50] and PDMS modulus with the increase of the temperature. We found that the imprinted depth reached its maximal value of 250 nm at 100 °C.

In addition to the vertical dimensions of the imprinted pattern, its lateral dimensions should be carefully examined, in order to verify that they do not undergo any distortion. Such distortion could stem, for instance, from the thermal expansion of hard PDMS features during the thermal imprinting. Unfortunately, we could not find any data on the thermal expansion coefficient of hard PDMS. The reported thermal expansion coefficient of soft PDMS is $\sim 3 \times 10^{-4}$–10^{-3} ($^{\circ}C^{-1}$), depending on the curing conditions.[54,55] According to this coefficient, the relative broadening of the imprinted features is $\frac{\Delta x}{x} = \alpha(100 - 25) \sim 2 - 7\%$. This calculation, however, is less relevant to our soft mold, in which the imaging features are made of hard PDMS. To experimentally estimate the possible effect of PDMS thermal expansion on the pattern transfer, we imaged both the master mold and the pattern imprinted at 100 °C using high-resolution SEM

(Fig. S5f and g, ESI†). We found that the grating periodicity and the line width are the same in the two samples (the little differences fell within the measurement error). Based on these findings, we conclude that the thermal expansion of hard PDMS is substantially lower than that of soft PDMS, and the possible impact of hard PDMS thermal expansion on the pattern transfer is negligible.

Fig. S7 (ESI†) shows 3D tilted SEM of an ultra-high-resolution pattern. Based on this image, the imprinted depth approximately corresponds to the height of the relief features on the soft mold, confirming that the pattern was fully transferred from the mold to the polymer. Also, Fig. S8 (ESI†) shows cross-sectional SEM of the imprinted grating. It can be roughly estimated from this image, taken at a tilt angle of 45°, that the imprinted depth was about 250 nm, which corresponds to the depth measured by AFM. In addition, we should note that the aspect ratio of the imprinted features did not exceed 1, which is also the limitation of most nanoimprinting approaches. Future work should be aimed at exploring the potential of soft thermal nanoimprinting to also produce high aspect-ratio nanostructures. The thickness of the imprinted resist can be arbitrarily varied by the concentration of the used resist solution and spinning speed, and can be easily fitted to the desired feature height, which should be, however, the same for all the features on the mold. Thus, if a mold contains differently sized features, they will have different aspect ratios. This is a general limitation of soft molds. On the other hand, master molds can be fabricated with features having different heights,[56] which can be, in principle, tuned to keep the same aspect ratio for differently sized features.

As mentioned above, one of the key advantages of soft nanoimprint molds over their rigid counterparts is that they can be used to imprint curved surfaces. Nanoimprinting of curved surfaces, in turn, paved the way to numerous applications impossible by conventional lithographic approaches, such as surface nano structuring of optical fibers,[18] as well as high throughput roll-to-roll nanoimprinting.[4,5] However, nanopatterning of curved surfaces using soft molds has been limited so far to UV imprinting. Here, we demonstrated the ultra-high-resolution nanoimprinting of a thermal resist onto a curved substrate using a PDMS mold. To that end, we coated a lens (a diameter of 30 mm and a radius of curvature of 50 mm) with a thin film of thermal resist. We then imprinted the resist using the same mold and process conditions as described for the imprinted flat substrates in Fig. 1. We found that the obtained imprinted pattern (Fig. 3), which contained critical dimensions down to 20 nm, is replicated onto the lens in a similar fashion to what was previously demonstrated for flat imprinted substrates. The simplicity and robustness of this process, together with its unprecedented 20 nm feature size, paves the way to nanopatterning of a large variety of thermoplastic materials onto substrates with unconventional geometries.

Up to now, we demonstrated applications of soft molds in the ultra-high-resolution thermal imprinting of thin polymer films. Another intriguing, yet much less explored, application of thermal nanoimprinting, is direct surface patterning with 3D nanostructures. Thermoplastic polymers are natural candidates for directly imprintable materials.[57] In addition, there has been emerging research exploring the direct nanopatterning of inorganic materials, such as chalcogenide glasses, whose relatively low glass transition point allows their imprinting at temperatures in the range of 100–200 °C.[58–61] Recently, we and others have demonstrated that the surface of chalcogenide glass can be directly imprinted with elastomeric molds without deforming the whole substrate.[33,62] However, imprinting of chalcogenide glasses has so far been demonstrated only for micron scale patterns.

Here, we demonstrate the direct thermal nano-imprinting of sub-20 nm relief features onto the surface of As_2Se_3 – chalcogenide glass with a glass transition temperature of 187 °C.[63] To allow direct thermal imprinting, we used a custom-made imprint setup (see the Experimental section) with an applied imprint temperature of 215 °C and pressure of 90 kPa. High-resolution SEM inspection of the imprinted surface (Fig. 4)

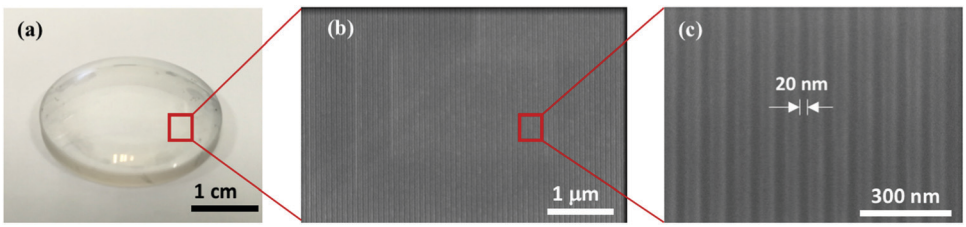

Fig. 3 (a) Optical image of the glass lens used as a substrate for nanoimprinting and (b) and (c) SEM of thermally nanoimprinted features on the lens spin coated with PBMA.

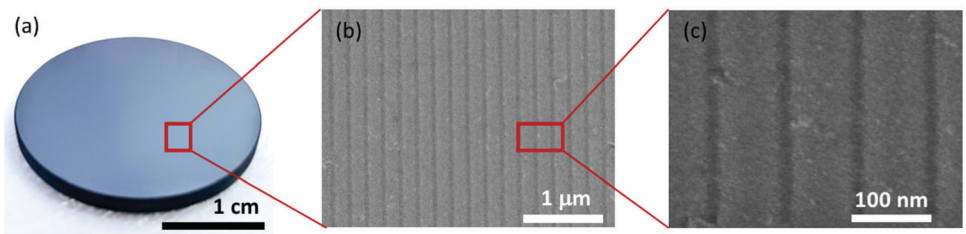

Fig. 4 (a) Substrate of As_2Se_3 used for direct thermal nanoimprinting and (b and c) SEM of the directly nanoimprinted As_2Se_3 substrate.

clearly shows that the relief pattern on the PDMS mold was completely transferred to the surface of the chalcogenide glass. Based on these images, the imprinted features seem to maintain their dimensions and shape, although a possible effect of thermal expansion of PDMS at such a high imprint temperature is to be studied in the future.

To summarize, we have demonstrated here a novel approach for soft thermal nanoimprinting with ultra-high resolution and feature size down to a 10 nm scale. We have shown that hybrid PDMS molds can be produced by two possible approaches: direct casting onto an electron-beam patterned organic positive-tone resist, and double-replication from a polymer patterned by a hard imprint mold. Each approach has its own unique advantages. The first approach is robust and facile, and allows straightforward mold replication without the need for the transfer of an electron-beam pattern onto the master substrate. The second approach takes advantage of the high-resolution of a HSQ resist, and its ability to structure rigid molding features after electron beam exposure. Both approaches ensure uniform feature height on the mold, which is tightly controlled by the thickness of the used electron beam resist. Furthermore, we demonstrated that the soft molds produced by our approaches are compatible with thermal nanoimprinting, and that by tuning the nanoimprint conditions, full pattern transfer and high pattern fidelity can be achieved. We also showed that thermal nanoimprinting with soft molds is a versatile nanofabrication process and can be used to pattern both flat and curved substrates. Finally, we showed that our nanoimprinting approach can be used for unique fabrication processes such as direct imprinting of chalcogenide glass.

Although features of 10 nm size scale demonstrated here can be produced today by extreme UV photolithography, which has recently been adopted by IC fabrication technology, such technology is very expensive, and is cost effective only for high-volume mass production. On the other hand, low volume production, research and development needs, and various niche applications still require non-standard lithographic approaches, which can be implemented with cheap and simple equipment and processes. Soft nanoimprint lithography largely addresses this requirement. Our findings push the boundaries of the miniaturization capabilities of soft nanoimprint lithography, and pave the way to numerous future applications which require robust and ultra-high resolution nanopatterning of standard, as well as unconventional, materials.

Conflicts of interest

The authors declare no conflicts of interest.

Acknowledgements

The authors thank Shay Joseph and Eviatar Kassiss from Optical Component Center, RAFAEL, for providing As_2Se_3 substrates. The work was funded by Israel Science Foundation, Individual Grant # 1401/15, Israel Science Foundations: F.I.R.S.T. Individual Grant # 2058/18, and Pazy Foundation Foundation – Israel Atomic Energy Commission.

References

1 S. Y. Chou, P. R. Krauss and P. J. Renstrom, *Appl. Phys. Lett.*, 1995, **67**, 3114.
2 S. Y. Chou, P. R. Krauss and P. J. Renstrom, *Science*, 1996, **272**, 85–87.
3 L. J. Guo, *J. Phys. D: Appl. Phys.*, 2004, 37.
4 S. H. Ahn and L. J. Guo, *ACS Nano*, 2009, **3**, 2304–2310.
5 S. H. Ahn and L. J. Guo, *Adv. Mater.*, 2008, **20**, 2044–2049.
6 T. Mårtensson, P. Carlberg, M. Borgström, L. Montelius, W. Seifert and L. Samuelson, *Nano Lett.*, 2004, **4**, 699–702.
7 L. J. Guo, *Adv. Mater.*, 2007, **19**, 495–513.
8 F. Hua, Y. Sun, A. Gaur, M. A. Meitl, L. Bilhaut, L. Rotkina, J. Wang, P. Geil, M. Shim, J. A. Rogers and A. Shim, *Nano Lett.*, 2004, **4**, 2467–2471.
9 W.-D. Li, W. Wu and R. Stanley Williams, *J. Vac. Sci. Technol., B: Nanotechnol. Microelectron.: Mater., Process., Meas., Phenom.*, 2012, **30**, 06F304.
10 W. Wu, W. M. Tong, J. Bartman, Y. Chen, R. Walmsley, Z. Yu, Q. Xia, I. Park, C. Picciotto and J. Gao, *Nano Lett.*, 2008, **8**, 3865–3869.
11 J. P. Rolland, E. C. Hagberg, G. M. Denison, K. R. Carter and J. M. De Simone, *Angew. Chem., Int. Ed.*, 2004, **43**, 5796–5799.
12 D. Qin, Y. Xia and G. M. Whitesides, *Nat. Protoc.*, 2010, **5**, 491–502.
13 H. Lan, *Updates in Advanced Lithography*, InTech, 2013.
14 Y. N. Xia and G. M. Whitesides, *Annu. Rev. Mater. Sci.*, 1998, **37**, 551–575.
15 H. Schmid and B. Michel, *Macromolecules*, 2000, **33**, 3042–3049.
16 T. W. Odom, J. C. Love, D. B. Wolfe, K. E. Paul and G. M. Whitesides, *Langmuir*, 2002, **18**, 5314–5320.
17 S. S. Williams, S. Retterer, R. Lopez, R. Ruiz, E. T. Samulski and J. M. Desimone, *Nano Lett.*, 2010, **10**, 1421–1428.
18 Z. Li, Y. Gu, L. Wangs, H. Ge, W. Wu, Q. Xia, C. Yuan, Y. Chen, B. Cui and R. S. Williams, *Nano Lett.*, 2009, **9**, 2306–2310.
19 D. G. Choi, J. H. Jeong, Y. S. Sim, E. S. Lee, W. S. Kim and B. S. Bae, *Langmuir*, 2005, **21**, 9390–9392.
20 K. M. Choi and J. A. Rogers, *J. Am. Chem. Soc.*, 2003, **125**, 4060–4061.
21 J. Zhang, B. Cui and H. Ge, *Microelectron. Eng.*, 2011, **88**, 2192–2195.
22 H. Becker and U. Heim, *Sens. Actuators, A*, 2000, **83**, 130–135.
23 Y. Yang, K. Mielczarek, M. Aryal, A. Zakhidov and W. Hu, *ACS Nano*, 2012, **6**, 2877–2892.
24 W. T. Neo, X. Li, S.-J. Chua, K. S. Ling Chong and J. Xu, *RSC Adv.*, 2017, **7**, 49119–49124.
25 Y. Yabiku, S. Kubo, M. Nakagawa, M. Vacha and S. Habuchi, *AIP Adv.*, 2013, **3**, 102128.
26 J. Kong, M. G. Chapline and H. Dai, *Adv. Mater.*, 2001, **13**, 1386–1389.
27 C. M. Bruinink, M. Péter, P. A. Maury, M. De Boer, L. Kuipers, J. Huskens and D. N. Reinhoudt, *Adv. Funct. Mater.*, 2006, **16**, 1555–1565.
28 D. Ho, J. Zou, B. Zdyrko, K. S. Iyer and I. Luzinov, *Nanoscale*, 2015, **7**, 401–414.

29 V. Bhingardive, L. Menahem and M. Schvartzman, *Nano Res.*, 2018, **11**, 2705–2714.
30 L. Menahem and M. Schvartzman, *J. Vac. Sci. Technol., B*, 2017, **35**, 010602.
31 H. Hauser, B. Herter, C. L. M. Hofmann, O. Höhn, V. Kübler, S. Fischer, S. Wolf, S. Fasold, F. C. J. M. van Veggel, J. C. Goldschmidt and B. Bläsi, *Microelectron. Eng.*, 2018, **187–188**, 154–159.
32 M. A. Verschuuren, M. Megens, Y. Ni, H. Van Sprang and A. Polman, *Adv. Opt. Technol.*, 2017, **6**, 243–264.
33 D. Yehuda, E. Kassis, S. Joseph and M. Schvartzman, *J. Vac. Sci. Technol., B*, 2018, **36**, 031602.
34 B. Bunday, A. Cepler, A. Cordes and A. Arceo, *Proc. SPIE*, 2013, **8861**, 86813B.
35 F. van Delft, R. van de Laar, M. Verschuuren, E. Platzgummer and H. Loeschner, *26th European Mask and Lithography Conference*, 2010, vol. 7545, p. 75450S.
36 C. Hedlund, H.-O. Blom and S. Berg, *J. Vac. Sci. Technol., A*, 1994, **2**, 1962.
37 M. Elwenspoek and H. V. Jansen, *Silicon Micormachining*, Cambridge University Press, 1998.
38 A. Cattoni, E. Cambril, D. Decanini, G. Faini and A. M. Haghiri-Gosnet, *Microelectron. Eng.*, 2010, **87**, 1015–1018.
39 M. Kawamori, K. Nakamatsu, Y. Haruyama and S. Matsui, *Jpn. J. Appl. Phys.*, 2006, **45**, 8994–8996.
40 M. D. Austin, H. Ge, W. Wu, M. Li, Z. Yu, D. Wasserman, S. A. Lyon and S. Y. Chou, *Appl. Phys. Lett.*, 2004, **84**, 5299.
41 D. Morecroft, J. K. W. Yang, S. Schuster, K. K. Berggren, Q. Xia, W. Wu and R. S. Williams, *J. Vac. Sci. Technol., B*, 2009, **27**, 2837–2840.
42 N. Koo, U. Plachetka, M. Otto, J. Bolten, J. H. Jeong, E. S. Lee and H. Kurz, *Nanotechnology*, 2008, **19**, 225304.
43 A. E. Grigorescu and C. W. Hagen, *Nanotechnology*, 2009, **20**, 292001.
44 V. R. Manfrinato, L. Zhang, D. Su, H. Duan, R. G. Hobbs, E. A. Stach and K. K. Berggren, *Nano Lett.*, 2013, **13**, 1555–1558.
45 N. Gadegaard and D. McCloy, *Microelectron. Eng.*, 2007, **84**, 2785–2789.
46 M. R. Saleem, P. A. Stenberg, M. B. Khan, Z. M. Khan, S. Honkanen and J. Turunen, *Advanced Fabrication Technologies for Micro/Nano Optics and Photonics V*, 2012, p. 82490G.
47 Y. Keydar, G. Le Saux, A. Edri, N. Bar-Hanin, E. Toledo, A. Pandey, V. Bhingardive, U. Hadad, A. Porgador and M. Schvartzman, *Nanoscale*, 2018, **10**, 14651–14659.
48 A. Marcovici, G. Le Saux, V. Bhingardive, P. Rukenstein, K. Flomin, K. Shreteh, R. Golan, T. Mokari and M. Schvartzman, *ACS Nano*, 2018, **12**, 10016–10023.
49 H. Schift and A. Kristensen, *Springer Handbook of Nanotechnology*, 2010, pp. 271–312.
50 H. Schift and L. J. Heyderman, in *Alternative Lithography*, ed. M. Sotomayor Torres Clivia, 2002, pp. 47–72.
51 Ò. D. Gordan, B. N. J. Persson, C. M. Cesa, D. Mayer, B. Hoffmann, S. Dieluweit and R. Merkel, *Langmuir*, 2008, **24**, 6636–6639.
52 J. M. Y. Carrillo and A. V. Dobrynin, *Langmuir*, 2009, **25**, 13244–13249.
53 S. Gilles, M. Diez, A. Offenhäusser, M. C. Lensen and D. Mayer, *Nanotechnology*, 2010, **21**, 245307.
54 B. E. Schubert and D. Floreano, *RSC Adv.*, 2013, **3**, 24671.
55 B. Kim, M. Park, Y. S. Kim and U. Jeong, *ACS Appl. Mater. Interfaces*, 2011, **3**, 4695–4702.
56 S. Ghassemi, N. Biais, K. Maniura, S. J. Wind, M. P. Sheetz and J. Hone, *J. Vac. Sci. Technol., B: Microelectron. Nanometer Struct.–Process., Meas., Phenom.*, 2008, **26**, 2549–2553.
57 Y. S. Seo and K. Park, *Microsyst. Technol.*, 2012, **18**, 2053–2061.
58 M. Solmaz, H. Park, C. K. Madsen and X. Cheng, *J. Vac. Sci. Technol., B*, 2008, **26**, 606–610.
59 T. Han, S. Madden, D. Bulla and B. Luther-Davies, *Opt. Express*, 2010, **18**, 19286–19291.
60 S. Danto, E. Koontz, Y. Zou, T. O. Ogbuu, B. Gleason, P. Peter Wachtel, J. D. Musgraves, J. Hu and K. Richardson, *Proc. SPIE*, 2013, **9884**, 88841T.
61 J. Orava, T. Kohoutek, L. Greer and H. Fudouzi, *Opt. Mater. Express*, 2011, **1**, 796–802.
62 M. R. Lotz, C. R. Petersen, C. Markos, O. Bang, M. H. Jakobsen and R. Taboryski, *Optica*, 2018, **5**, 557–563.
63 D. W. Henderson and D. G. Ast, *J. Non-Cryst. Solids*, 1984, **64**, 43–70.

